Watanabe Y, Sachiko Horie, Funaki Y, Kikuchi Y, Yamazaki H, Ishii K, Mori S, Vassaux G, Kodama T.	Delivery of Na/I symporter gene into skeletal muscle by using nanobubbles and ultrasound: Visualization of gene expression by positron emission tomography.	Journal of Nuclear Medicine (in press)			2009

国際会議での発表

発表者氏名	論文タイトル名	学会・研究会名	巻号	ページ	開催日	開催地
Keiichi Saito, Shiro Mori, Masao Ono, Takeyoshi Koseki	Immunohistochemical localization of CD134 ligand, CD137 ligand, GITR ligand and BAFF in Sjogren's syndrome-like autoimmune sialadenitis of MRL/lpr mice (P41).	The 3rd International Symposium for Interface Oral Health Science in SENDAI			1/15-1/16/2009	Sendai International Center, Sendai, Japan.
Li L, Horie S, Chen R, Watanabe Y, Sakamoto M, Mori S, Takahashi S, Kodama T.	Three-dimentional high-frequency ultrasound imaging for early diagnosis of lymph node metastasis combined with microbubbles.	The 3rd East Asian Pacific Student Workshop on Nano-Biomedical Engineering.			Dec. 21-22, 2009	Engineering Auditorium, National University Of Singapore, Singapore.
Li L, Chen R, Horie S, Watanabe Y, Baba T, Sax N, Sakamoto M, Mori S, Takahashi S, Kodama T.	Ultrasound molecular imaging of lymph node metastasis with nano/microbubbles.	International Symposium of AIDS and Tuberculosis (ISAT2010)			January 13-14, 2010, n	Sendai, Japan.
Sax N, Horie S, Li L, Chen R, Watanabe Y, Mori S, Kodama T.	Physical characterization of acoustic liposomes.	International Symposium of AIDS and Tuberculosis (ISAT2010)			January 13-14, 2010,	Sendai, Japan.
Horie S, Watanabe Y, Chen R, Mori S, Matsumura Y, Kodama T.	Targeted gene delivery using nanobubble and ultrasound.	The 5th International Symposium on Medical, Bio- and Nano-Electronics.	Book of Abstract.	115-16.	Febrary 24-25,2010,	Sendai, Japan.

Watanabe Y, Horie S, Funaki Y, Kikuchi Y, HYamazaki H, Ishii K, Mori S, Kodama T.	PET imaging of Na/I symporter gene expression induced by nanobubbles and ultrasound.	The 5th International Symposium on Medical, Bio- and Nano-Electronics.	Book of Abstract.	111-112.	Febrary 24-25,2010,	Sendai, Japan.
Chen R, YWatanabe Y, Li L, Horie S, Mori S, Fukumoto M, Kodama T.	Observation for angiogenesis of liver metastases in preclinical models.	The 5th International Symposium on Medical, Bio- and Nano-Electronics.	Book of Abstract.	113-114.	Febrary 24-25,2010,	Sendai, Japan.
Li L, Horie S, Rui CHEN, Watanabe Y, Baba T, Sax N, Sakamoto M, Mori S, Takahashi S, Kodama T.	Four-dimensional high-frequency ultrasound imaging system for early detection of lymph node micro-metastasis.	The 5th International Symposium on Medical, Bio- and Nano-Electronics.	Book of Abstract.	157-158.	Febrary 24-25,2010,	Sendai, Japan.
Sax N, Horie S, Li L, Chen R, Watanabe Y, Mori S, Kodama T.	TEM observation and analysis of echogenic nano-bubbles.	The 5th International Symposium on Medical, Bio- and Nano-Electronics.	Book of Abstract.	159-160.	Febrary 24-25,2010,	Sendai, Japan.
Yagishita Y, Takata Y, Ohki K, Miyashita H, Morikawa H, Sakamoto M, Mori S,Kawamura H , Kodama T.	Volumetric and angiogenetic imaging system by using nanobubbles and high-frequency ultrasound for evaluation of the antitumor effect by cisplatin.	The 5th International Symposium on Medical, Bio- and Nano-Electronics.	Book of Abstract..	161-162	Febrary 24-25,2010,	Sendai, Japan.

国内会議での発表

発表者氏名	論文タイトル名	学会・研究会名	巻号	ページ	開催日	開催地
高田陽子, 森 士朗, 小枝聡子, 川村 仁, 伊達文子, 小野栄夫	関節強直症マウスのゲノム解析と顎変形症疾患モデル動物としての可能性についての検討	第19回日本顎変形症学会総会			2009年6月4-5日	仙台
森 士朗, 李 麗, 堀江佐知子, 渡邊夕紀子, 大木宏介, 宮下 仁, 川村 仁, 森川秀広, 小玉哲也	ナノバブルと超音波を用いた口腔癌リアルタイム画像診断システムの開発に向けての検討	第33回日本頭頸部癌学会			2009年6月11-12日	札幌

宮下 仁, 森 士朗, 李 麗, 堀江佐知子, 渡邊夕紀子, 大木宏介, 川村 仁, 森川秀広, 小玉哲也	ナノバブルと超音波を用いた抗腫瘍分子導入システムによる抗腫瘍効果に関する検討	第33回日本頭頸部癌学会			2009年6月11-12日	札幌
大木宏介, 森 士朗, 李 麗, 堀江佐知子, 渡邊夕紀子, 宮下 仁, 川村仁, 森川秀広, 小玉哲也	ナノバブルと超音波を用いた口腔癌画像診断システムの診断精度に関する検討	第33回日本頭頸部癌学会			2009年6月11-12日	札幌
森 士朗, 李 麗, 堀江佐知子, 渡邊夕紀子, 大木宏介, 宮下 仁, 川村 仁, 森川秀広, 小玉哲也	ナノバブルと超音波を用いた口腔癌診断システムの遠隔地医療への応用(口外)	第35回(社)日本口腔外科学会北日本地方会			009年6月26-27日	旭川
李麗, 冨田典子, 森士朗, 大澤ふき, 堀江佐知子, 陳鋭, 渡辺夕紀子, 阪本真弥, 高橋昭喜, 小玉哲也	ナノバブルを用いたリンパ節転移診断に関する三次元高周波超音波イメージング法の開発	日本機械学会第21回バイオエンジニアリング講演会	講演論文集	71-72頁	2009年1月23日-24日	札幌コンベンションセンター
李麗, 堀江佐知子, 陳鋭, 渡辺夕紀子, 阪本真弥, 高橋昭喜, 森士朗, 小玉哲也	リンパ節転移早期診断に関する三次元高周波超音波イメージング	日本超音波医学会 東北地方会 第37回学術集会	プログラム・抄録集	1頁	2009年3月15日	仙台市情報・産業プラザ
堀江佐知子, 渡邊夕紀子, 陳鋭, 李麗, 森士朗, 小玉哲也	表在性膀胱がんに対する新しい遺伝子治療法の開発	日本超音波医学会 東北地方会 第37回学術集会	プログラム・抄録集	5頁	2009年3月15日	仙台市情報・産業プラザ
堀江佐知子, 渡邊夕紀子, 陳鋭, 李麗, 森士朗, 小玉哲也	表在性膀胱がんへの遺伝子治療法の開発	第48回日本生体医工学会大会	第47巻特別号プログラム・抄録集	222頁	2009年4月23-25日	タワーホール船堀(東京)
陳鋭, 渡邊夕紀子, 堀江佐知子, 森士朗, 福本学, 小玉哲也	床試験を目指した肝転移モデルの非侵襲的観察	本機械学会2009年度年次大会	講演論文集Vol.6.	117-118頁	2009年9月13日-16日	岩手大学
森 士朗, 高田陽子, 大木宏介, 宮下 仁, 川村 仁, 森川秀広, 小玉哲也	ナノバブルと高周波超音波画像診断装置の遠隔地口腔診断への応用	第54回(社)日本口腔外科学総会			2009年10月9-11日	札幌
高田陽子, 森 士朗, 小枝聡子, 川村 仁, 丹田奈緒子	新しい関節強直症モデルマウスのゲノム解析	第54回(社)日本口腔外科学総会			2009年10月9-11日	札幌

別紙３

厚生労働科学研究費補助金（医療機器開発推進研究事業）
（総括・分担）研究報告書

阻害剤の細胞膜への導入に関する分子動力学シミュレーション

分担研究者　藤川　重雄　北海道大学大学院工学研究科教授

研究要旨　衝撃波の脂質二重層膜(DPPC)通過に伴う膜の変形機構を調べることを目的として、衝撃波を分子動力学(MD)法で計算するための非平衡・非定常 MD 法を開発し、衝撃波通過後に、ナノ秒の時間スケールで膜を貫く水孔が自発的に形成されること、水孔の形成過程と形成条件、水孔内部での５FU 分子の拡散過程を明らかにした。また、上記の結果を実証するための基礎研究を目的として、脂質気泡群を含む液体中での超音波の音響減衰スペクトル測定を行い、気泡群の共振周波数は 1.2MPa であること、この周波数で気泡群が崩壊される可能性を明らかにした。

Ａ．研究目的

本研究は、以下の二つの課題に関する基礎研究を目的としてなされたものである。

(1) 微細気泡から放射される衝撃波によるがん細胞内への阻害剤の導入機構を調べるために、非平衡・非定常 MD シミュレーションにより、(i) ピコ秒の時間スケールでの脂質二重層膜(DPPC)の構造変化、(ii) ピコ秒の時間スケールでの膜構造の変化後のナノ秒の時間スケールでの膜構造の変化、(iii) 膜の影響による５FU 分子の拡散運動等を調べる。

(2) 脂質二重層膜変形の上記の結果を実証するための基礎研究を行い、脂質気泡群(DSPC)を含む液体中での超音波の音響減衰スペクトル測定から、気泡群の共振周波数を調べる。

Ｂ．研究方法

(1) 細胞膜の基本構造である脂質二重層膜を、脂質分子(DPPC)と水分子を用いて MD 法によってコンピュータ上に作成し、この膜に衝撃波を作用させて膜の構造変化を調べた。膜が動的に変形する機構および阻害剤（水分子と５FU 分子の２種類で模擬）の導入プロセスをスーパーコンピュータにより分子レベルで解析した。

(2) 八フッ化プロパン(C_3F_8)を含むナノスケールの脂質気泡群(DSPC)を対象として、液体中で気泡群に広帯域周波数の超音波を照射し、気泡群の存在による音波の減衰を測定し、気泡群の共振周波数について検討した。（倫理面への配慮）コンピュータ解析であるため特別な配慮はしなかった。

Ｃ．研究結果と考察

(1) 衝撃波による膜構造の変化は、急激な崩壊と穏やかな回復の二つの段階に分かれることがわかった。膜構造の回復段階において、衝撃波の通過によって増加した脂質分子の側方向の流動性は弱くなることなく、この流動性の増加と同時に、水分子が膜疎水領域へ定常的に導入される。上記の結果に基づき、脂質膜の疎水領域に水分子を挿入した状態を初期条件として平衡 MD 計算を行い、膜疎水領域への水分子の導入により、３ナノ秒内に水孔が自発的に形成され、その水孔の形成率とサイズは導入する水分子の数の増加とともに増加する。さらに、抗がん剤分子の水孔通過機構を調べるために、バルクな水中と脂質膜に挟まれた水中での、抗がん剤としての５FU 分子の MD シミュレーションを行い、脂質膜近傍では５FU 分子の拡散係数が小さくなることを明らかにした。

(2) 脂質気泡群に広帯域周波数の超音波を照射実験に関しては、音響減衰スペクトルは 1.2MHz 付近にピークが存在し、脂質濃度が高いほど減衰が大きくなることが明らかになった。この結果は、脂質気泡群が 1.2MHz 程度で最も効果的に崩壊することを示唆するものである。

Ｄ．結論

(1) 衝撃波通過後に、ナノ秒の時間スケールで膜を貫く水孔が自発的に形成され、その水孔の形成率とサイズは挿入する水分子の数の増加とともに増加する。

(2) ５FU 分子が水孔を通過するためには、半径５nm の水孔が１０ns 間存在すればよく、脂質膜近傍では５FU 分子の拡散係数が小さくなる。

(3) 脂質気泡群による音響スペクトル減衰は 1.2MHz 付近でピークを示し、脂質濃度が高いほど減衰が大きくなる。この結果は脂質気泡群が 1.2MHz 程度で最も効果的に崩壊することを示唆している。

Ｅ．研究発表

１．論文発表

(1) R. Imai, H. Nakagawa, T. Kanagawa, M. Watanabe, S. Fujikawa, Acoustic Characteristics of Ultrasound in Water Containing Lipid Microbubbles, Proc. of 7th World Conf. on Exp. Heat Transf., Fluid Dynamics and Thermodynamics, Poland, (2009-7), pp.223-228.

(2) T. Kanagawa, T. Yano, M. Watanabe, S. Fujikawa, Dispersive Waves in Mixtures of Liquid and Gas Bubbles based on a Two-Fluid Model, Proc. of 7th Int. Symp. on Cavitation, USA, (2009-8), pp.1-10.

他３編.

別紙

研究成果の刊行に関する一覧表

雑誌

発表者氏名	論文タイトル名	発表誌名	巻号	ページ	出版年
R. Imai H. Nakagawa T. Kanagawa M. Watanabe S. Fujikawa	Acoustic Characteristics of Ultrasound in Water Containing Lipid Microbubbles	Proc. of 7th World Conf. on Exp. Heat Transf., Fluid Dynamics and Thermodynamics (Poland)	CD-ROM	pp.223-228	2009
T. Kanagawa T. Yano M. Watanabe S. Fujikawa	Weakly Nonlinear Analysis of Dispersive Waves in Mixtures of Liquid and Gas Bubbles Based on a Two-Fluid Model	Proc. of 7th Int. Symp. on Cavitation (USA)	CD-ROM	pp.1-10	2009
今井亮介 中川浩哉 桜井康介 渡部正夫 藤川重雄	脂質気泡群を含む液体中を伝播する超音波の音響特性	日本機械学会年次大会講演論文集)	CD-ROM	pp.1-2	2009
金川哲也 矢野　猛 渡部正夫 藤川重雄	気泡流中における準単色波の弱非線形伝播	日本流体力学会年会2009講演論文集	CD-ROM	pp.1-4	2009
金川哲也 矢野　猛 渡部正夫 藤川重雄	気泡流中の弱非線形波動	京都大学数理解析研究所考究録	CD-ROM	pp.1-7	2009

研究成果の刊行に関する一覧表

別紙

研究成果の刊行に関する一覧表

雑誌

発表者氏名	論文タイトル名	発表誌名	巻号	ページ	出版年
R. Chen, M. Chiba, S. Mori, M. Fukumoto, T. Kodama.	Periodontal Gene Transfer by Ultrasound and Nano-/Microbubbles.	J Dent Res	88(11)	1008-1013	2009
Han F, Takeda K, Ishikawa K, Ono M, Date F, Yokoyama S, Furuyama K, Shinozawa Y, Urade Y, Shibahara S.	Induction of lipocalin-type prostaglandin D synthase in mouse heart under hypoxemia.	Biochemical and Biophysical Research Communication	385	449-53	2009
R. Imai H. Nakagawa T. Kanagawa M. Watanabe S. Fujikawa	Acoustic Characteristics of Ultrasound in Water Containing Lipid Microbubbles	Proc. of 7th World Conf. on Exp. Heat Transf., Fluid Dynamics and Thermodynamics (Poland)	CD-ROM	pp.223-228	2009
今井亮介 中川浩哉 桜井康介 渡部正夫 藤川重雄	脂質気泡群を含む液体中を伝播する超音波の音響特性	日本機械学会年次大会講演論文集)	CD-ROM	pp.1-2	2009
金川哲也 矢野 猛 渡部正夫 藤川重雄	気泡流中における準単色波の弱非線形伝播	日本流体力学会年会2009講演論文集	CD-ROM	pp.1-4	2009
金川哲也 矢野 猛 渡部正夫 藤川重雄	気泡流中の弱非線形波動	京都大学数理解析研究所考究録	CD-ROM	pp.1-7	2009
T. Kanagawa T. Yano M. Watanabe S. Fujikaw	Weakly Nonlinear Analysis of Dispersive Waves in Mixtures of Liquid and Gas Bubbles Based on a Two-Fluid Model	Proc. of 7th Int. Symp. on Cavitation (USA)	CD-ROM	pp.1-10	2009

Kaneko I, Suzuki K, Matsuo K, Kumagai H, Owada Y, Noguchi N, Hishinuma T, Ono M.	Cysteinyl leukotrienes enhance the degranulation of bone marrow-derived mast cells through the autocrine mechanism.	Tohoku J Exp Med	217	185-91	2009
Kodama T, Tomita N, Horie S, Sax N,Iwasaki H, Suzuki R, Maruyama K, Mori S, Fukumoto M.	Morphological study on acoustic liposome using transmission electron microscopy	Journal of Electron Microscopy			2009
Kodama T, Tomita Y, Watanabe Y, Koshiyama K, Yano T, Fujikawa S.	Cavitation bubbles mediated molecular delivery during sonoporation	Journal of Biomechanical Science and Engineering	4	124-140	2009
Hiroaki Komori, Yoshiko Soga, Shiro Mori, Masato Nose.	Genetic Analysis of Arsenic Toxicities Using an Experimental Mouse Model. In Chemical Pollution in Indochina; Contamination Status, Ecosystem Impact and Remediation Technology. Ed. By Satoru Suzuki and Hideshige Takada.	Tokai University Press		160-167	2009
Suzuki R, Oda Y, Utoguchi N, Namai E, Taira Y, Okada N, Kadowaki N, Kodama T, Tachibana K, Maruyama K.	A novel strategy utilizing ultrasound for antigen delivery in dendritic cell-based cancer immunotherapy	Journal of Controlled Release	133	198-205	2009

Yuki Tanaka, Hiroaki Komori, Shiro Mori, Yoshiko Soga, Takahito Tsubaki, Miho Terada, Tatsuhiko Miyazaki, Takahiro Fujino, Satoshi Nakamura, Hiroyuki Kanno, Tatsuya Sawasaki, Yaeta Endo, Masato Nose	Evaluating the Role of Rheumatoid Factors for the Development of Rheumatoid Arthritis in a Mouse Model with a Newly Established ELISA System.	The Tohoku Journal of Experimental Medicine.	220 (3)	199-206	2010
Watanabe Y, Sachiko Horie, Funaki Y, Kikuchi Y, Yamazaki H, Ishii K, Mori S, Vassaux G, Kodama T.	Delivery of Na/I symporter gene into skeletal muscle by using nanobubbles and ultrasound: Visualization of gene expression by positron emission tomography	Journal of Nuclear Medicine			2010 in press
柳下陽子, 小玉哲也.	音響性リポソームと超音波を利用した遺伝子薬物デリバリー	血管医学	10-4	91-98	2009
Yamashita M, Iwama N, Date F, Chiba R, Ebina M, Miki H, Yamauchi K, Sawai T, Nose M, Sato S, Takahashi T, Ono M.	Characterization of lymphangiogenesis in various stages of idiopathic diffuse alveolar damage.	Hum Pathology	40	542-51	2009
Yamashita M, Yamauchi K, Chiba R, Iwama N, Date F, Shibata N, Kumagai H, Risteli J, Sato S, Takahashi T, Ono M.	The definition of fibrogenic processes in fibroblastic foci of idiopathic pulmonary fibrosis based on morphometric quantification of extracellular matrices.	Hum Pathology	40	1278-87	2009

研究成果の刊行物・別刷

RESEARCH REPORTS
Biomaterials & Bioengineering

R. Chen[1], M. Chiba[2], S. Mori[3], M. Fukumoto[4], and T. Kodama[1]*

[1]Molecular Delivery System Laboratory, Department of Biomedical Engineering, Graduate School of Biomedical Engineering, Tohoku University, 2-1 Seiryo-machi, Aoba-ku, Sendai 980-8575, Japan; [2]Division of Oral Physiology, Graduate School of Dentistry, Tohoku University, Japan; [3]Tohoku University Hospital, Sendai, Japan; and [4]Department of Pathology, Institute of Development, Aging, and Cancer, Tohoku University, Japan; *corresponding author, kodama@bme.tohoku.ac.jp

J Dent Res 88(11):1008-1013, 2009

Periodontal Gene Transfer by Ultrasound and Nano/Microbubbles

ABSTRACT

A non-viral gene delivery approach with nano/microbubbles and ultrasound offers opportunities for targeting soft tissues for gene therapy. The periodontium is a complex structure comprised of hard (cementum, alveolar bone) and soft tissues (periodontal ligament, gingivae). We hypothesized that our established gene delivery method would allow the periodontal tissue to be targeted for transfection for gene therapy. Expression kinetics and sites of transfection sites with this approach were investigated in rat periodontal tissue. Bioluminescence imaging revealed that transient gene expression was induced at day 1 post-transfection, while confocal microscopy showed that gene expression was localized in the muscle cells of gingival tissues. These findings indicate that regular transfection with this approach results in high gene expression, facilitating gene therapy for periodontal disease involving alveolar bone resorption.

KEY WORDS: gene therapy, ultrasound, membrane permeability, periodontal tissues, non-viral vector.

INTRODUCTION

Periodontal disease is characterized by the inflammation of periodontal tissues, which eventually leads to the loss of alveolar bone and teeth. Several tissue-engineering techniques have been developed over time and are considered to be promising for the restoration of lost periodontal structure (Mussig *et al.*, 2005; Ramseier *et al.*, 2006; Moioli *et al.*, 2007). Until now, single administration of purified tissue growth factors has not been shown to be clinically effective, due to proteolytic degradation, rapid diffusion, and solubility of the delivery vehicle (Pradeep and Karthikeyan, 2003). Gene transfer methods may circumvent many of the limitations associated with protein delivery (Blesing and Kerr, 1996; Ramseier *et al.*, 2006); however, progress in experimental and clinical periodontal gene therapy is limited by the immunogenicity and cytotoxicity of viral vectors and low transfection efficiency with regard to non-viral vectors (Nishida *et al.*, 2006). It has recently been reported that therapeutic ultrasound (US) in combination with echo contrast agents such as nano/microbubbles (NBs) can facilitate gene transfection *in vitro* and *in vivo* (Taniyama *et al.*, 2002a,b; Bekeredjian *et al.*, 2003; Dijkmans *et al.*, 2004; Shimamura *et al.*, 2004; Nishida *et al.*, 2006; Takahashi *et al.*, 2007; Aoi *et al.*, 2008). This physical method has several advantages, such as low toxicity, low immunogenicity, non-invasiveness, high target selectivity, and repeated applicability (Bekeredjian *et al.*, 2005). The periodontium is a complex structure comprised of hard (cementum, alveolar bone) and soft tissues (periodontal ligament, gingivae). We hypothesized that our established gene delivery method allows the periodontal tissue to be targeted for transfection for gene therapy. In the present study, we investigated the functional gene expression profile, localized sites, and target cells transfected by the delivery of two kinds of reporter genes [firefly luciferase and EGFP (enhanced green fluorescent protein) genes], using the method we developed. We used bioluminescence imaging and confocal microscopy to determine the kinetics of transient gene expression and localized gene expression sites, respectively.

MATERIALS & METHODS

This study was approved by the Animal Care Committee of Tohoku University.

Nano/Microbubbles

Lipid bubbles were created in an aqueous dispersion of 2 mg/mL 1,2-distearoyl-sn-glycero-3-phosphocholine (Avanti Polar Lipids, Alabaster, AL, USA) and

DOI: 10.1177/0022034509346119

Received September 18, 2008; Last revision June 9, 2009; Accepted June 12, 2009

1 mg/mL polyethylene glycol 40 stearate (Sigma-Aldrich Co., St. Louis, MO, USA), with the use of a 20-kHz sonicator (Vibra Cell; Sonics & Materials Inc., Danbury, CT, USA) in the presence of octafluoropropane gas. The peak diameter was 1272 ± 163 nm, which we evaluated by measuring the size distribution of lipid bubbles with a laser diffraction particle size analyzer (ELSZ-2; Otsuka Electronics Co. Ltd., Osaka, Japan) (Aoi *et al.*, 2008).

Plasmid Preparation

Two different expression vector plasmid DNAs encoding firefly luciferase (simian virus 40 promoter-driven pGL3-control vector; Promega Corp., Madison, WI, USA) and enhanced green fluorescent protein (EGFP, simian virus 40 promoter-driven pEGFP-N1 vector; Clontech, Palo Alto, CA, USA) were used. The plasmids were grown in *Escherichia coli* host strain JM109 (Promega), purified with a QIAGEN plasmid isolation kit (QIAGEN, Hilden, Germany), and prepared at a final concentration of 1 mg/mL.

Periodontal Tissue Transfection by Ultrasound and Nano/Microbubbles

Six-week-old male Wistar rats were divided into 4 groups: DNA alone (n = 6), DNA + US (n = 6), DNA + NB (n = 7), and DNA + US + NB (n = 10). The rats were anesthetized with an intraperitoneal injection of 5% sodium pentobarbital (40 mg/kg). A mixture of 10 μL pGL-3 plasmid and lipid bubbles at a final concentration of 50% (v/v) was injected into the labial periodontal tissue of the upper incisors by means of a 27-gauge stainless steel needle. Immediately after injection, the rats were exposed to US insonation for 1 min at the injection location, which was covered with US gel (Aquasonic; Parker Laboratories Inc., Fairfield, NJ, USA). A US-emitting transducer (diameter, 6 mm; frequency, 950 KHz; intensity, 3.0 W/cm^2; exposure time, 60 sec; and duty cycle, 20%; Fuji Ceramics Co., Fujinomiya, Japan) was used for US insonation. After insonation, the rats were kept under a heat lamp until recovery from the anesthesia.

Analysis of Transfected Gene Expression

After 1 day of periodontal tissue transfection, each rat was anesthetized with pentobarbital and intraperitoneally injected with luciferin (150 mg/kg of body weight; Promega). After 15 min of luciferin administration, luciferase bioluminescence was quantified for 5 min in an *in vivo* imaging system (Xenogen Corp., Alameda, CA, USA). Half the number of rats in each group (DNA alone, n = 3; DNA + US, n = 3; DNA + NB, n = 3; and DNA + US + NB, n = 5) were then randomly selected and raised as usual after recovery from the anesthesia. These rats were further observed on days 3 and 5 and then killed by excessive ether. The other rats were also killed by excessive ether. The upper jaws with the incisors were dissected, fixed in 4% paraformaldehyde in phosphate-buffered saline (PBS) overnight, decalcified with 10% ethylenediaminetetraacetic acid for 7 wks at 4°C, dehydrated, and then embedded in paraffin. The embedded specimens were cut into 6-μm serial coronal or sagittal sections and stained with hematoxylin and eosin.

Ex vivo Detection of Transgene Expression by an *in vivo* Imaging System

The luciferase gene was transferred to the periodontal tissues of 3 rats by US and NBs, by the same procedure and conditions described above. After 24 hrs, transfected gene expression was detected by luciferase bioluminescence imaging for 5 min after the luciferin injection. The labial gingivae of maxillary incisors were then dissected and placed on a six-well plate completely covered with 30 mg luciferin in 1 mL PBS. Bioluminescence of the removed gingivae and the rats from which they were removed was immediately quantified for 1 min. After observation, the rats were killed by excessive ether.

Confocal Microscopic Observation of EGFP Expression

Periodontal EGFP gene transfection was performed with US and NBs. The rats (n = 4) were killed by excessive ether 24 hrs post-transfection. The upper jaws with the incisors were removed, embedded in 5% carboxymethyl cellulose gel, and frozen in hexane-dry ice (Kawamoto and Shimizu, 2000). The frozen blocks were attached to the sample stage of a cryomicrotome (CM 3500; Leica Instruments, Heidelberg, Germany) kept in a cryochamber (–25°C). Serial coronal sections (7 μm thick) were collected and fixed in 4% paraformaldehyde for 10 min and then incubated in a 1.5-μM propidium iodide staining solution in the dark for 30 min. EFGP and propidium iodide distribution patterns were directly observed by confocal microscopy (FV-1000; Olympus, Tokyo, Japan).

Statistical Analysis

The values are expressed as means ± standard deviation (SD). Data were analyzed for statistical differences by a one- or two-way analysis of variance (ANOVA) and the Tukey-Kramer test. Differences of $P < 0.05$ were considered significant.

RESULTS

All the rats survived the experimental procedure and showed excellent recovery. No significant deficits in eating and drinking functions, no abnormal mobility of the incisors, and no appreciable macroscopic changes at the injection site were observed. Body weights of the rats that completed the whole experiment (DNA alone, n = 3; DNA + US, n = 3; DNA + NB, n = 3; and DNA + US + NB, n = 5) were analyzed. The rats in all the groups showed similar weight growth curves (Fig. 1A). Their body weight increased throughout the experimental period, except at day 1 post-transfection, when no obvious increase was observed. There were no significant differences among the groups either before or after gene transfer ($P > 0.05$).

We investigated the effectiveness of the use of US and NBs in periodontal gene transfer. The luciferase activities in the periodontal tissues were determined at day 1 after the 4 treatments: DNA alone (n = 6), DNA + US (n = 6), DNA + NB (n = 7), and

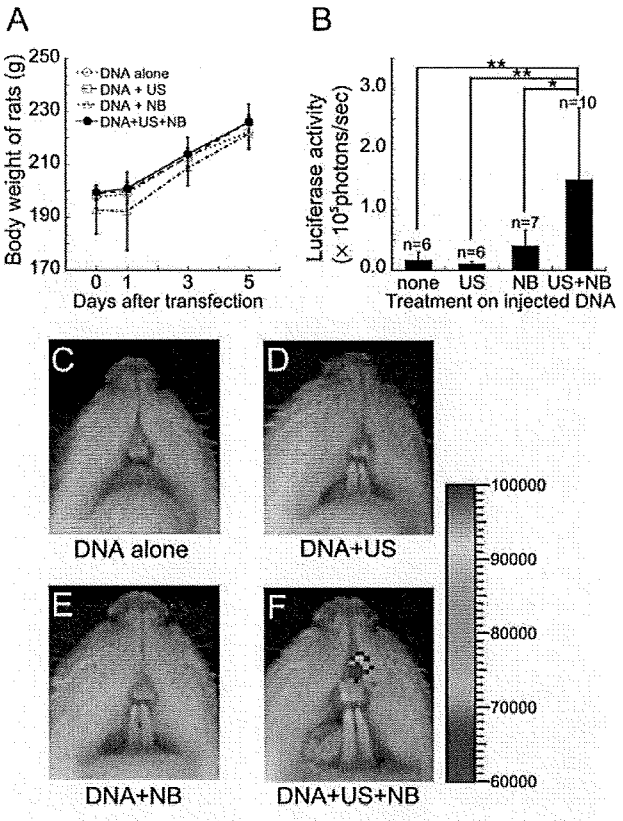

Figure 1. Effects of ultrasound (US) and nano/microbubbles (NBs) on periodontal gene transfer. Rats were divided into 4 groups: DNA alone, DNA + US, DNA + NB, and DNA + US + NB. The US parameters were as follows: central frequency, 950 kHz; duty cycle, 20%; number of pulses, 200; intensity, 3.0 W/cm^2; and exposure time, 60 sec. NBs: lipid bubbles. **(A)** Rats' body weights in each group immediately before and 1, 3, and 5 days post-transfection. No significant differences ($P > 0.05$) were found between each of the two groups in the same time period. N = 3 for groups DNA alone, DNA + US, and DNA + NB, while n = 5 for group DNA + US + NB. Data are presented as means ± SD. **(B)** Luciferase activity at day 1 post-transfection revealed the efficiency of gene delivery in each group. There were no significant differences among the control groups (DNA alone, n = 6; DNA + US, n = 6; and DNA + NB, n = 7; $P > 0.05$). Sonication after DNA + NB injection (*i.e.*, DNA + US + NB treatment, n = 10) significantly increased the luciferase activity compared with the other groups. *$P < 0.05$, ** $P < 0.01$. Data are presented as means ± SD. **(C–F)** Representative images of luciferase bioluminescence in the labial periodontal tissues of the rats' maxillary incisors for DNA alone (C), DNA + NB (D), DNA + US (E), and DNA + US + NB (F). Color bar units represent photons/s/cm^2.

DNA + US + NB (n = 10) (Fig. 1B). The luciferase activities in the DNA+NB and DNA+US treatments were as low as that with the DNA alone treatment ($P > 0.05$). In contrast, ultrasonication after the DNA + NB injection significantly increased luciferase activity compared with the other 3 treatments ($P < 0.05$). Representative images of bioluminescence in the labial periodontal tissues of the rats' maxillary incisors for the 4 different treatments are shown in Figs. 1C–1F.

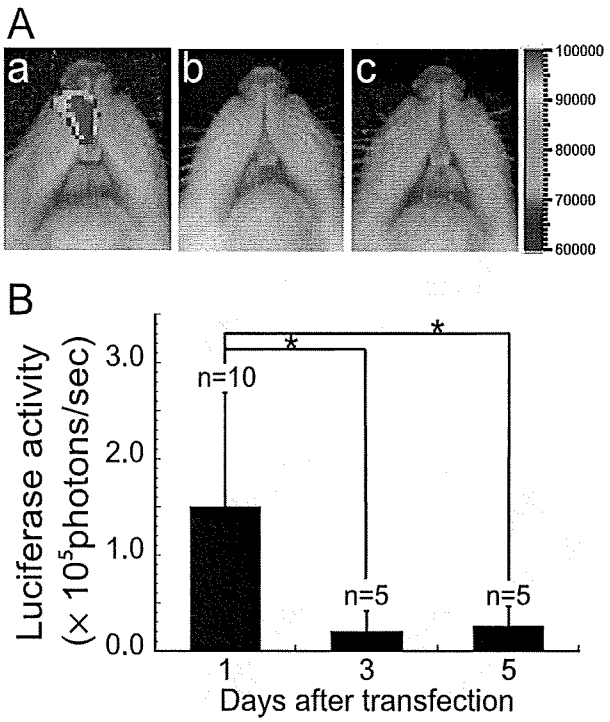

Figure 2. Time-course of gene expression in periodontal tissues after gene transfection by US and NBs. **(A)** Representative images showing luciferase gene expression in the labial periodontal tissues of the upper incisors of rat on (a) day 1 (n = 10), (b) day 3 (n = 5), and (c) day 5 (n = 5). Color bar units represent photons/sec/cm^2. **(B)** Luciferase activity with elapsed time. Gene expression disappeared 3 days post-transfection by the US-NB method. * $P < 0.05$. Data are presented as means ± SD.

We next investigated the kinetics of gene expression for the DNA + US + NB group (Figs. 2A, 2B). The day-1 luciferase activity decreased to a background level ($P < 0.05$; Fig. 2B) at day 3, which was similar to the results of other treatments (data not shown).

To identify the specific gene expression sites, after confirming the luciferase gene expression in the periodontal tissues at day 1 post-transfection (Fig. 3A), we removed the gingivae of the rats. The rats whose gingivae were removed exhibited weak luciferase activity in the labial tissues of the maxillary incisors (Fig. 3B), while the extracted gingivae showed strong luciferase activity (Fig. 3C, arrow). From *ex vivo* observation, we concluded that the expression sites were mainly localized in the gingival tissues.

Histological observation showed no hemorrhage or inflammation (Figs. 4A, 4B), while fluorescence images showed that EGFP expression was mostly confined to the labial gingival tissues of the maxillary incisors (Figs. 4C, 4E, 4G). The nuclei of EGFP-positive cells were located in the peripheral aspect of the cell, just under the plasma membrane. This is a typical histological feature of skeletal muscle cells in transverse section. Therefore, we considered the cells that expressed EGFP to be muscle cells in the gingival tissues (Figs. 4D, 4F, 4H).

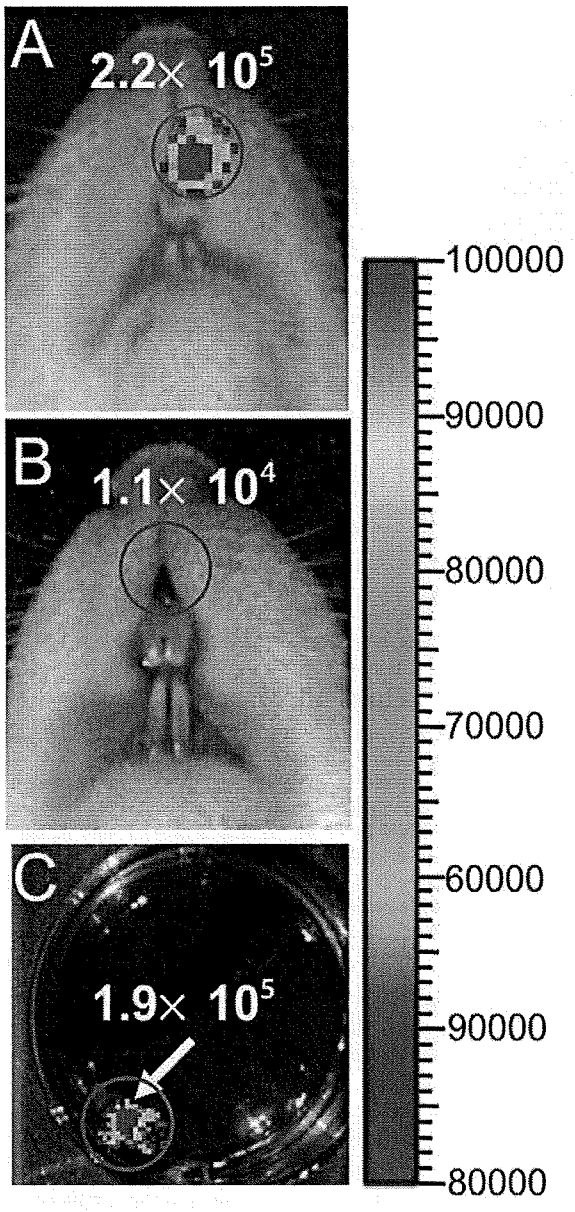

Figure 3. Site of expression of the gene transfected by US and NBs *ex vivo* shown by means of an *in vivo* imaging system. **(A)** After luciferase, gene expression (2.2×10^5 photons/sec) in the labial periodontal tissues of the rats' upper incisors was detected at day 1 post-transfection. The labial gingivae adjacent to the upper incisors were removed and placed on a six-well plate completely covered with 30 mg luciferin in 1 mL phosphate-buffered saline. **(B)** The rats whose gingivae were removed expressed very weak luciferase activity (1.1×10^4 photons/sec) in the labial tissues of the maxillary incisors. **(C)** The excised gingivae showed strong luciferase activity (1.9×10^5 photons/sec, arrow). Color bar units represent photons/sec/cm^2.

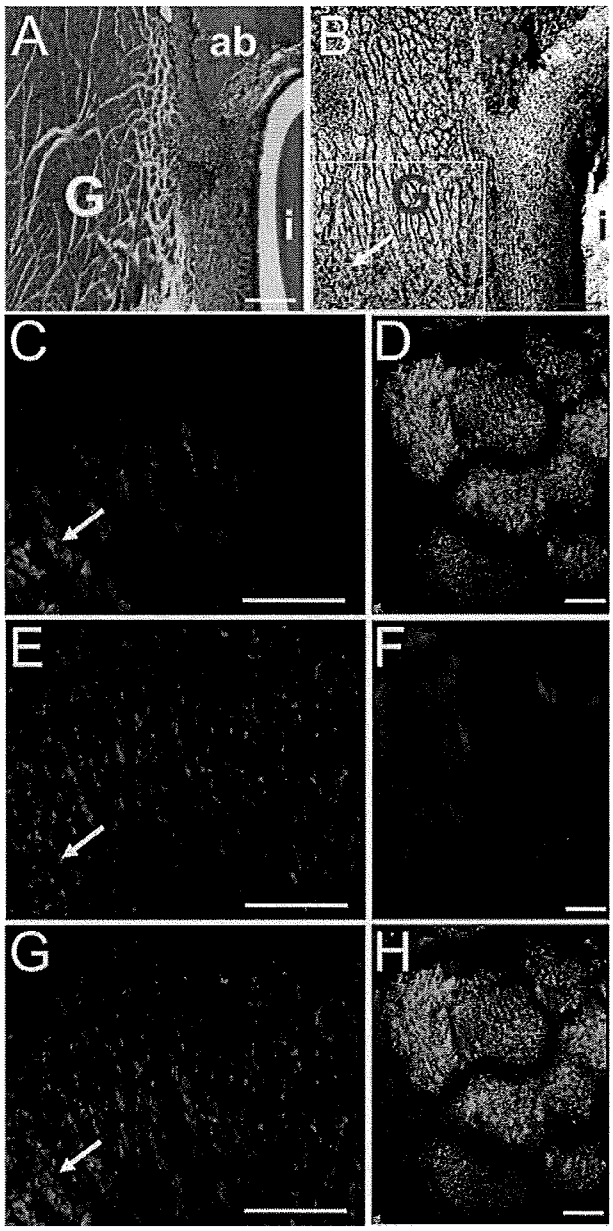

Figure 4. Histology of the rat's periodontal tissues after gene delivery by US and NBs. **(A)** Hematoxylin and eosin staining in the decalcified sections of the rat's upper jaws with incisors 1 day after luciferase gene delivery. **(B)** Transmission image of the undecalcified frozen section of the rat's upper jaws with incisors 1 day after enhanced green fluorescent protein (EGFP) was transferred. No hemorrhage or inflammation was detected. **(C-H)** Fluorescence images of the undecalcified frozen section. EGFP expression was mostly confined to the muscle cells in the gingivae of the labial periodontal tissues. **(C)** EGFP expression in (B) (yellow square); **(D)** image of C at higher magnification (arrow); **(E)** propidium-iodide-stained red nuclei in (B) (yellow square); **(F)** image of E at higher magnification (arrow); **(G)** composite overlay fluorescence images of EGFP and nuclei in (B) (arrow); and **(H)** image of G at higher magnification (arrow). i, incisors; ab, alveolar bone; g, gingiva. Scale bars in A, B, C, E, and G = 100 μm. Scale bars in D, F, and H = 10 μm.

DISCUSSION

The present study clearly demonstrated that the exposure of periodontal tissues injected with a mixture of plasmid DNAs

and lipid bubbles to US facilitated luciferase gene transfection into the rat periodontal tissues. No significant systemic or localized abnormality was observed after the procedures. To the best of our knowledge, this is the first report on the *in vivo* transfection of periodontal tissues by the non-virus-mediated method described above.

It has been suggested that the mechanical forces generated by the collapse of either NBs or cavitation bubbles by ultrasonication induce transient permeabilization of cells (Kodama *et al.*, 2000, 2005; Lawrie *et al.*, 2000; Guzmán *et al.*, 2002). Along with NBs, ultra-short US field pulses ($\leq$ 10 μs) are required to avoid irreversible membrane permeability (van Wamel *et al.*, 2006). Therefore, 1.05-μs (950 KHz) US-generating transducers were used in this study. Furthermore, since cell viability decreases with increasing exposure to energy (Guzmán *et al.*, 2002), a comparatively low energy (36 J/cm^2) was used for the periodontal gene transfer.

In the present *in vivo* study, increased gene expression was detected in the periodontal tissues of the rats' upper incisors at day 1 after transfection. Gene expression dramatically reduced at day 3, highlighting the transient nature of US/NB-mediated gene transfer. The results demonstrate that US-mediated destruction of NBs loaded with plasmid DNA is a feasible and efficient technique for local gene delivery within periodontal tissues. The transient expression is likely to be the result of rapid plasmid DNA degradation for the abundant blood stream in the delivery site. Modulated gene expression profile delivered every one or two days was considered to be useful for the maintenance of high gene expression. US is a well-established diagnostic and therapeutic tool in medicine. Furthermore, NBs are used in clinical situations, and plasmid DNA is less immunogenic and much easier to prepare (Nishida *et al.*, 2006). Therefore, repeated application of the above technique should be feasible and safe.

Gene expression in the excised gingival tissues was determined *ex vivo* by an *in vivo* imaging system. This expression was further confirmed by EGFP expression. It is known that fibroblasts are the most abundant cells in human gingival tissues. However, in this study, muscle cells were found in rat gingival tissues. The initiation of adequate periodontal regeneration may be assisted by an array of growth factors, such as platelet-derived growth factor and bone morphogenetic proteins (Moioli *et al.*, 2007). Gingival fibroblasts express various cytokines, which play important roles in the pathogenesis of inflammation-induced bone resorption (Okada and Murakami, 1998; Belibasakis *et al.*, 2005; Palmqvist *et al.*, 2008). For example, it has been reported that platelet-derived growth factor genes transduced gingival fibroblasts and enhanced periodontal defects by induction of human gingival fibroblast migration and proliferation (Ramseier *et al.*, 2006). Transgene expression in the gingival tissues could be beneficial for inhibiting alveolar bone absorption in periodontitis with the technique described in this paper. Indeed, while complex gene delivery systems are becoming more and more attractive, research in this area is still in its infancy (Ramseier *et al.*, 2006; Moioli *et al.*, 2007). Periodontal gene delivery by US and NBs can easily make complex gene delivery a reality (Pitt *et al.*, 2004).

It should be noted that the relatively short duration of gene expression was a limitation of this study. Since the membrane properties and physical characteristics of NBs are associated with the efficiency of gene transfection, the possible utility and safety of NBs other than lipid bubbles (*e.g.*, acoustic liposomes) for periodontal gene transfer remain to be investigated in the future. The present US-NB approach has the potential to prolong the duration of transgene expression by optimizing acoustic parameters (Kodama *et al.*, 2006) and developing a periodontal-tissue-specific US probe. Additionally, since the functional expression of genes transfected into periodontal tissues has not been examined thus far, further efforts with therapeutic genes are needed to investigate the clinical utility of the US-NB approach.

In conclusion, the present approach may be beneficial for periodontal gene therapy because of advantages such as minimal invasiveness, regional targetability, and possible paracrine delivery of therapeutic molecules associated with the alveolar bone.

ACKNOWLEDGMENTS

We thank Yukiko Watanabe, Sachiko Horie, and Noriko Tomita for their technical assistance. T. Kodama received a Grant-in-Aid for Scientific Research (B) (20300173), Grants-in-Aid for Scientific Research on Priority Area, from the Ministry of Education, Culture, Sports, Science, and Technology (MEXT) of Japan (20015005); and a Grant for Research on Advanced Medical Technology from the Ministry of Health, Labor, and Welfare of Japan (H19-nano-010). M. Chiba received a Grant-in-Aid for Scientific Research (B) (16390602). S. Mori received a Grand-in-Aid for Scientific Research (B) (19390507). R. Chen received Grants-in-Aid for JSPS Fellowship.

REFERENCES

Aoi A, Watanabe Y, Mori S, Takahashi M, Vassaux G, Kodama T (2008). Herpes simplex virus thymidine kinase-mediated suicide gene therapy using nano/microbubbles and ultrasound. *Ultrasound Med Biol* 34:425-434.

Bekeredjian R, Chen S, Frenkel PA, Grayburn PA, Shohet RV (2003). Ultrasound-targeted microbubble destruction can repeatedly direct highly specific plasmid expression to the heart. *Circulation* 108:1022-1026.

Bekeredjian R, Grayburn PA, Shohet RV (2005). Use of ultrasound contrast agents for gene or drug delivery in cardiovascular medicine. *J Am Coll Cardiol* 45:329-335.

Belibasakis GN, Johansson A, Wang Y, Chen C, Lagergard T, Kalfas S, *et al.* (2005). Cytokine responses of human gingival fibroblasts to *Actinobacillus actinomycetemcomitans* cytolethal distending toxin. *Cytokine* 30:56-63.

Blesing CH, Kerr DJ (1996). Intra-hepatic arterial drug delivery. *J Drug Target* 3:341-347.

Dijkmans PA, Juffermans LJ, Musters RJ, van Wamel A, ten Cate FJ, van Gilst W, *et al.* (2004). Microbubbles and ultrasound: from diagnosis to therapy. *Eur J Echocardiogr* 5:245-256.

Guzmán HR, Nguyen DX, McNamara AJ, Prausnitz MR (2002). Equilibrium loading of cells with macromolecules by ultrasound: effects of molecular size and acoustic energy. *J Pharm Sci* 91:1693-1701.

Kawamoto T, Shimizu M (2000). A method for preparing 2- to 50-micron-thick fresh-frozen sections of large samples and undecalcified hard tissues. *Histochem Cell Biol* 113:331-339.

Kodama T, Hamblin MR, Doukas AG (2000). Cytoplasmic molecular delivery with shock waves: importance of impulse. *Biophys J* 79:1821-1832.

Kodama T, Tan PH, Offiah I, Partridge T, Cook T, George AJ, *et al.* (2005). Delivery of oligodeoxynucleotides into human saphenous veins and the adjunct effect of ultrasound and microbubbles. *Ultrasound Med Biol* 31:1683-1691.

Kodama T, Tomita Y, Koshiyama K, Blomley MJ (2006). Transfection effect of microbubbles on cells in superposed ultrasound waves and behavior of cavitation bubble. *Ultrasound Med Biol* 32:905-914.

Lawrie A, Brisken AF, Francis SE, Cumberland DC, Crossman DC, Newman CM (2000). Microbubble-enhanced ultrasound for vascular gene delivery. *Gene Ther* 7:2023-2027.

Moioli EK, Clark PA, Xin X, Lal S, Mao JJ (2007). Matrices and scaffolds for drug delivery in dental, oral and craniofacial tissue engineering. *Adv Drug Deliv Rev* 59:308-324.

Mussig E, Tomakidi P, Steinberg T (2005). Molecules contributing to the maintenance of periodontal tissues. Their possible association with orthodontic tooth movement. *J Orofac Orthop* 66:422-433.

Nishida K, Doita M, Takada T, Kakutani K, Miyamoto H, Shimomura T, *et al.* (2006). Sustained transgene expression in intervertebral disc cells in vivo mediated by microbubble-enhanced ultrasound gene therapy. *Spine* 31:1415-1419.

Okada H, Murakami S (1998). Cytokine expression in periodontal health and disease. *Crit Rev Oral Biol Med* 9:248-266.

Palmqvist P, Lundberg P, Lundgren I, Hánström L, Lerner UH (2008). IL-1beta and TNF-alpha regulate IL-6-type cytokines in gingival fibroblasts. *J Dent Res* 87:558-563.

Pitt WG, Husseini GA, Staples BJ (2004). Ultrasonic drug delivery–a general review. *Expert Opin Drug Deliv* 1:37-56.

Pradeep AR, Karthikeyan BV (2003). Tissue engineering: prospect for regenerating periodontal tissues. *Indian J Dent Res* 14:224-229.

Ramseier CA, Abramson ZR, Jin Q, Giannobile WV (2006). Gene therapeutics for periodontal regenerative medicine. *Dent Clin North Am* 50: 245-263.

Shimamura M, Sato N, Taniyama Y, Yamamoto S, Endoh M, Kurinami H, *et al.* (2004). Development of efficient plasmid DNA transfer into adult rat central nervous system using microbubble-enhanced ultrasound. *Gene Ther* 11:1532-1539.

Takahashi M, Kido K, Aoi A, Furukawa H, Ono M, Kodama T (2007). Spinal gene transfer using ultrasound and microbubbles. *J Control Release* 117:267-272.

Taniyama Y, Tachibana K, Hiraoka K, Aoki M, Yamamoto S, Matsumoto K, *et al.* (2002a). Development of safe and efficient novel nonviral gene transfer using ultrasound: enhancement of transfection efficiency of naked plasmid DNA in skeletal muscle. *Gene Ther* 9:372-380.

Taniyama Y, Tachibana K, Hiraoka K, Namba T, Yamasaki K, Hashiya N, *et al.* (2002b). Local delivery of plasmid DNA into rat carotid artery using ultrasound. *Circulation* 105:1233-1239.

van Wamel A, Kooiman K, Harteveld M, Emmer M, ten Cate FJ, Versluis M, *et al.* (2006). Vibrating microbubbles poking individual cells: drug transfer into cells via sonoporation. *J Control Release* 112:149-155.

Biochemical and Biophysical Research Communications 385 (2009) 449–453

Contents lists available at ScienceDirect

Biochemical and Biophysical Research Communications

journal homepage: www.elsevier.com/locate/ybbrc

Induction of lipocalin-type prostaglandin D synthase in mouse heart under hypoxemia

Feng Han [a,b,1], Kazuhisa Takeda [a], Kazunobu Ishikawa [c], Masao Ono [d], Fumiko Date [d], Satoru Yokoyama [a], Kazumichi Furuyama [a], Yotaro Shinozawa [b], Yoshihiro Urade [e], Shigeki Shibahara [a,*]

[a] Department of Molecular Biology and Applied Physiology, Tohoku University School of Medicine, Sendai 980-8575, Japan
[b] Department of Emergency and Critical Care Medicine, Tohoku University School of Medicine, Sendai 980-8575, Japan
[c] First Department of Internal Medicine, Fukushima Medical University, Fukushima, Japan
[d] Division of Histopathology, Graduate School of Medicine, Tohoku University, Sendai 980-8575, Japan
[e] Department of Molecular Behavioral Biology, Osaka Bioscience Institute, Osaka, Japan

ARTICLE INFO

Article history:
Received 13 May 2009
Available online 24 May 2009

Keywords:
Prostaglandin D synthase
Heme oxygenase
Hypoxia
Prostaglandin D_2
Lung
Heart
Pulmonary venous myocardium

ABSTRACT

Hypoxemia is a common manifestation of various disorders and generates pressure overload to the heart. Here we analyzed the expression of lipocalin-type prostaglandin D synthase (L-PGDS) in the heart of C57BL/6 mice kept under normobaric hypoxia (10% O_2) that generates hemodynamic stress. Northern and Western blot analyses revealed that the expression levels of L-PGDS mRNA and protein were significantly increased (>twofold) after 14 days of hypoxia, compared to the mice kept under normoxia. Immunohistochemical analysis indicated that L-PGDS was increased in the myocardium of auricles and ventricles and the pulmonary venous myocardium at 28 days of hypoxia. Moreover, using C57BL/6 mice lacking heme oxygenase-2 (HO-$2^{-/-}$), a model of chronic hypoxemia, we showed that the expression level of L-PGDS protein was twofold higher in the heart than that of wild-type mouse. L-PGDS expression is induced in the myocardium under hypoxemia, which may reflect the adaptation to the hemodynamic stress.

Introduction

Hypoxemia is a common manifestation of various disorders, including sleep apnea syndrome and chronic obstructive lung diseases. Chronic hypoxemia causes the remodeling of the pulmonary artery that is characterized by proliferation of vascular smooth muscle cells and may increase pulmonary vascular resistance [1,2], thereby causing pulmonary hypertension. Pulmonary hypertension could generate pressure overload to the right ventricle, which eventually leads to heart failure. Among various disorders, the ventilation–perfusion mismatching is the most common mechanism that causes hypoxemia [3].

Lipocalin-type prostaglandin (PG) D synthase (L-PGDS) catalyzes the isomerization of PGH_2 to produce PGD_2 [4] and also functions as a lipophilic ligand-binding protein for various small hydrophobic substances, such as biliverdin, bilirubin, and retinoic acid [5]. L-PGDS therefore functions as a PGD_2-producing enzyme and a secreted carrier protein [4]. L-PGDS is expressed in the central nervous system [6,7], retina [8,9], melanocytes [9], heart [10], and male and female genital organs [4,11]. L-PGDS is secreted into the coronary circulation from the myocardium, and accumulates in the coronary circulation of angina patients [10,12]. L-PGDS is localized in human myocardial cells, atrial endocardial cells, smooth muscle cells in the arteriosclerotic intima, and the atherosclerotic plaque of coronary arteries [10]. In this connection, it has been reported that fluid shear stress increases the expression of L-PGDS in vascular endothelial cells [13,14]. In primary pulmonary hypertension, urinary PGD_2 metabolites were increased [15]. Moreover, the increase in serum L-PGDS was reported in patients with obstructive sleep apnea syndrome complicating excessive daytime sleepiness [16]. It is therefore conceivable that expression of L-PGDS may be regulated in a dynamic manner under hemodynamic stress.

Heme oxygenase-2-deficient (HO-$2^{-/-}$) mice exhibit mild hypoxemia, which may be the consequence of ventilation–perfusion mismatching [17]. In fact, HO-$2^{-/-}$ mice show the thickening of the pulmonary venous myocardium [17] and the enlargement of the carotid body [18]. These morphometric changes are attributable to chronic hypoxemia [19]. HO-$2^{-/-}$ mice therefore may

* Corresponding author. Address: Department of Molecular Biology and Applied Physiology, Tohoku University School of Medicine, 2-1 Seiryo-machi, Aoba-ku, Sendai, Miyagi 980-8575, Japan. Fax: +81 22 717 8118.
E-mail address: shibahar@mail.tains.tohoku.ac.jp (S. Shibahara).
[1] Present address: Department of Anesthesiology, Beijing Jishuitan Hospital, 31 Xinjiekou East Street, Xicheng District, Beijing 100035, China.

0006-291X/$ - see front matter © 2009 Elsevier Inc. All rights reserved.
doi:10.1016/j.bbrc.2009.05.092

provide a unique model of hypoxemia or ventilation–perfusion mismatching. HO-2 and the structurally related isozyme, heme oxygenase-1 (HO-1), are essential in heme catabolism, each of which also plays an important role in cellular homeostasis [3,20]. Recently, we have reported that PGD_2 induces HO-1 expression in cultured human cell lines [21,22], which suggests the regulatory link between heme catabolism and the L-PGDS/PGD_2 system [23].

As a first step to explore the role of L-PGDS in the cardiopulmonary tissues, we analyzed its expression using two mouse models of chronic hypoxemia: C57BL/6 mice lacking HO-2 (HO-$2^{-/-}$) maintained under normoxia [17] and wild-type C57BL/6 mice during acclimatization to normobaric hypoxia (10% O_2 under barometric pressure at the sea level) [24]. Here we describe the induction of L-PGDS expression in the heart as a response to hemodynamic stress.

Methods

Animal treatment. HO-$2^{-/-}$ mice on the C57BL/6 background were generated [25] and were maintained as previously described [17]. Male C57BL/6 mice (5 weeks old) were obtained from the Animal Experimental Center of Tohoku University School of Medicine (Sendai, Japan) and were housed for one week before the beginning of the study. Mice were randomly selected into two groups, as described previously [24]. One group of mice was maintained in a normobaric hypoxic chamber with 10% O_2 for 1, 3, 5, 7, 14, 21, or 28 days ($n = 3$ for each group), as detailed previously [24,26]. The barometric pressure was kept at the sea-level value. The age-matched control mice were kept under normoxia (room air) in the same room, in which the hypoxic chamber was placed. At the end of the exposure, the animals were anesthetized with diethyl

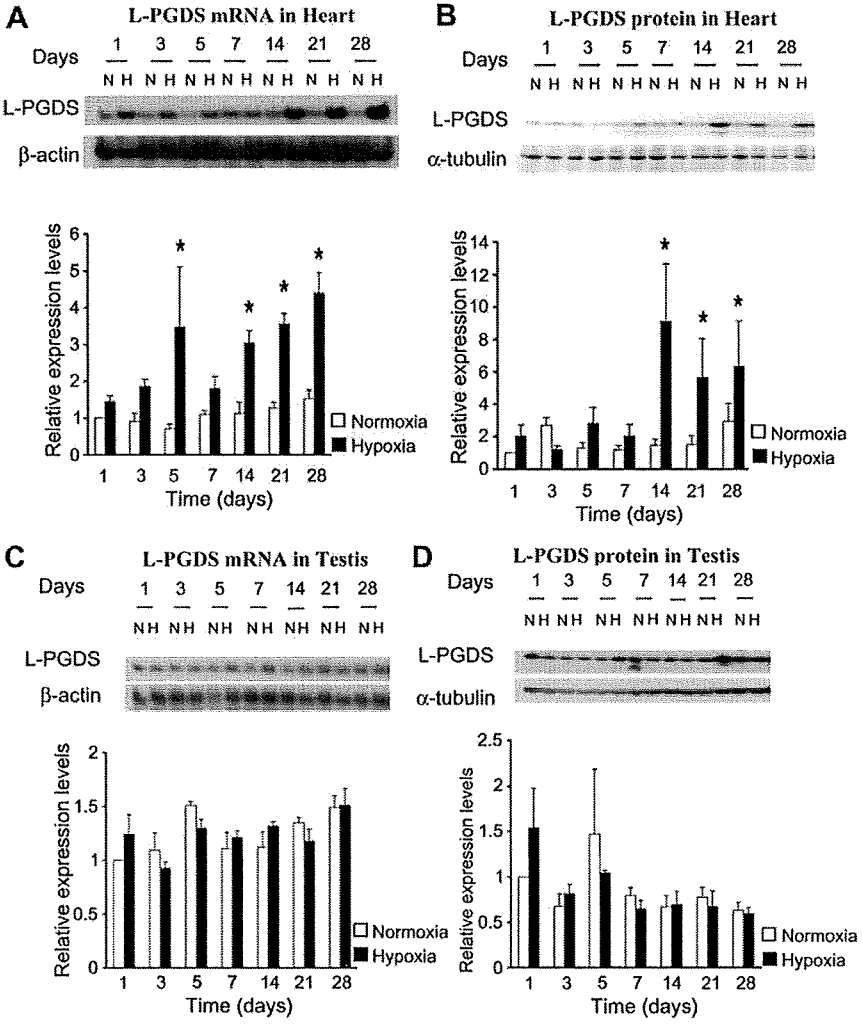

Fig. 1. Expression profiles of L-PGDS mRNA and protein in the heart and testis during hypoxia. (A,C) Northern blot analysis. The heart and testis tissues were isolated from mice after exposure to hypoxia for the indicated time or age-matched control. Total RNAs were extracted from each tissue sample, and then subjected to Northern blot analysis (top panel). Each lane contains 20 μg of total RNA. The lanes labeled N and H contained RNA prepared from mice maintained under normoxia and hypoxia, respectively. The expression level of β-actin mRNA is shown as an internal control. The data shown are from one of three independent experiments with similar results. The intensities of the signals in the Northern blots were normalized with respect to the intensity for β-actin. The bottom panel shows the relative expression level of L-PGDS mRNA, which represents the ratio of each normalized value under normoxia (open column) or hypoxia (closed column) to that of the age-matched control mice, kept under normoxia for 1 day. Asterisks represent statistically significant difference compared to the normoxia value at 1 day ($^*p < 0.05$). (B,D) Western blot analysis. Tissue extracts were prepared from the heart and testis and analyzed by Western blot analysis with a rabbit polyclonal anti-mouse L-PGDS antibody (top panel). Each lane contains 20 μg protein. The data shown are from one of three independent experiments with similar results. The same filter was used for anti-α-tubulin monoclonal antibody. The intensities of the signals in the Western blots were normalized with respect to the intensity for α-tubulin (internal control). The relative expression level of L-PGDS protein indicates the ratio of each normalized value to that of the control mice kept for 1 day under normoxia (bottom panel). Asterisks represent statistically significant difference compared to the normoxia value at 1 day ($^*p < 0.05$).

ether, and the lung, heart, and testis were isolated. All animal experiments were performed based on the institutionally approved protocols of Tohoku University School of Medicine and Fukushima Medical University.

Northern blot analysis. Total RNA was extracted from the lung, heart, and testis and subjected to Northern blot analysis, as detailed previously [27]. The northern probe used for L-PGDS mRNA was the mouse L-PGDS cDNA fragment containing the entire protein-coding region (Accession No. X8922) [9]. The expression of β-actin mRNA was examined as an internal control [24,27]. These DNA fragments were labeled with [α-^{32}P] dCTP (Amersham Biosciences) by the random primer method and were used as hybridization probes, as described previously [27].

Western blot analysis. Tissue extracts were prepared from the hearts and lungs of wild-type mice exposed to normoxia or hypoxia, as detailed previously [24]. Tissue extracts were also prepared from the testes and hearts of HO-2$^{-/-}$ mice (10 weeks old) and age-matched wild-type mice. Each tissue sample was homogenized on ice in cold triple detergent lysis buffer [24,28]. Western blots were incubated with a rabbit polyclonal anti-mouse L-PGDS antibody [29]. The treatment with the primary antibody was performed for 1 h at room temperature or overnight at 4 °C for L-PGDS antibody at a dilution of 1:20,000 in Tris-buffered saline with 0.1% Tween 20 and 1% non-fat milk. In some cases, the membranes (Western blots) were incubated with a rabbit polyclonal antibody against rat HO-1 [30] or mouse HO-2 (SPA-897, StressGen Biotechnologies Corp., Canada), as detailed previously [24]. The specific immunocomplexes were detected with a Western blot kit (ECL Plus, Amersham Biosciences). Expression of α-tubulin was determined as an internal control with α-tubulin antibody (Neo Markers, CA, USA).

Morphological analysis of the pulmonary vasculatures. Isolated hearts and lungs were fixed in 4% paraformaldehyde and paraffin-embedded. Deparaffinized lung sections were stained by elastica-Masson staining method to evaluate the wall thickness and elastic lumina. Pathological changes of the small pulmonary arteries were assessed by the microscopic examination, as previously reported [31].

Immunohistochemistry. Paraffin-embedded tissues were sectioned at 2.5 μm in thickness. Deparaffinized sections were digested with 0.1% trypsin in 0.1% $CaCl_2$ for 30 min at room temperature to retrieve immunoreactivity and then immunohistochemical study was performed on the tissue sections using a standard labeled streptavidin–biotin method (Nichirei, Tokyo, Japan). Rabbit polyclonal anti-mouse L-PGDS antibody [29] was used at a 1:2000 dilution. Nuclei on the tissue sections were visualized with hematoxylin.

Statistical analysis. Experimental data from each group are expressed as means ± SEM. All results are derived from three animals per group. Statistical analyses were performed with two-way analysis of variance (factorial design) with a post hoc comparison test

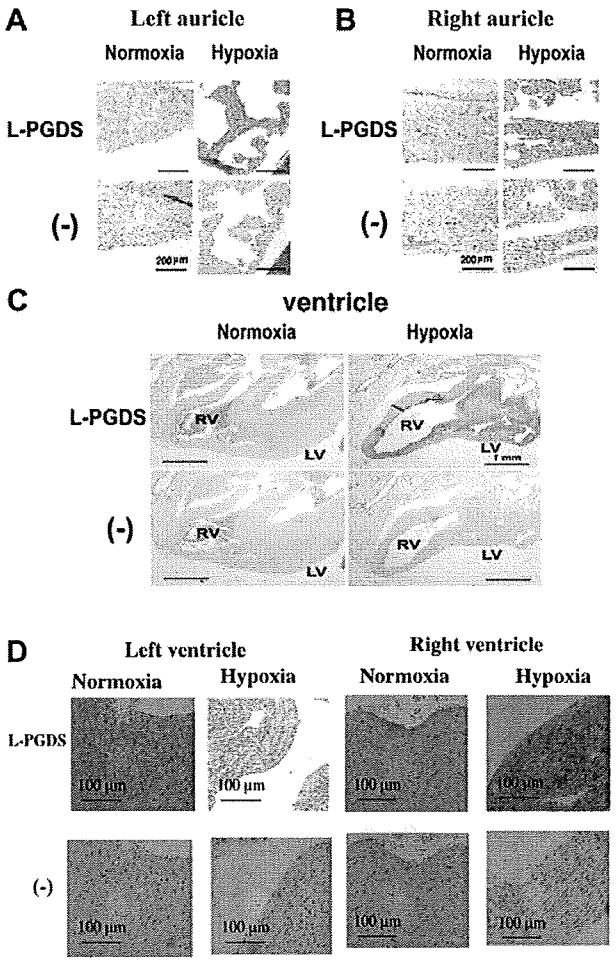

Fig. 2. Expression of L-PGDS protein in the myocardium is increased under hypoxia. Tissue sections were prepared from mouse heart exposed to hypoxia or normoxia for 28 days, and were reacted with anti-L-PGDS antibody or control serum. (A) Expression of L-PGDS in the left auricle under normoxia (left panels) and hypoxia (right panels). (B) Expression of L-PGDS in the right auricle. (C) Expression of L-PGDS in left ventricle (LV) and right ventricle (RV). (D) Eight panels show the large magnification of ventricles shown in (c).

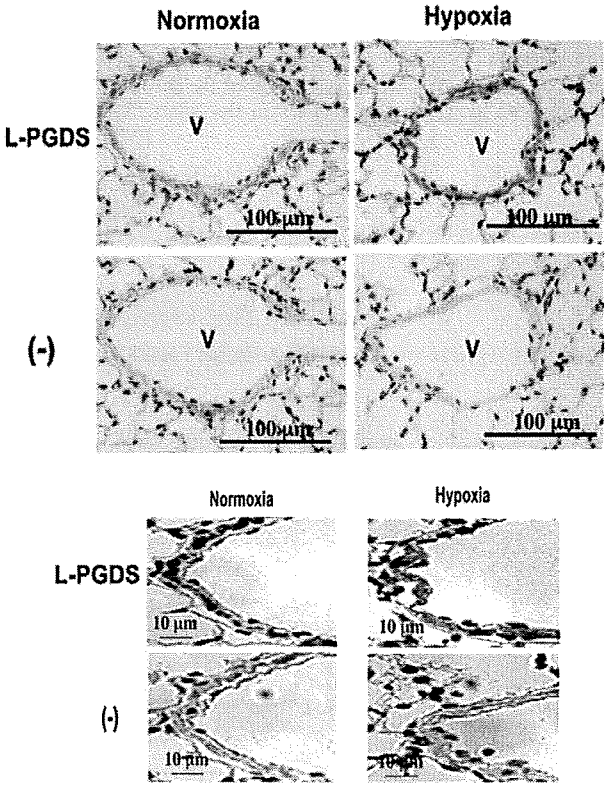

Fig. 3. L-PGDS protein increased in the pulmonary venous myocardium. The lung was isolated from mice exposed to hypoxia or normoxia for 28 days. Tissue sections were reacted with anti-L-PGDS antibody or control serum. V indicates the pulmonary vein. Lower panels show the large magnification of the pulmonary vein.

(Fisher's Protected Least Significant Difference exact test) with commercially available software (Statview 4.0, Carabasas, CA). Differences between mean values were considered significant when $p < 0.05$.

Results and discussion

Expression profiles of L-PGDS in the heart during normobaric hypoxia

We reported that C57BL/6 mice exhibited increased numbers of red blood cells and increased hematocrit during acclimatization to normobaric hypoxia (10% O_2) [24]. We also confirmed the remodeling of the pulmonary vasculatures after 28 days of normobaric hypoxia; namely, the vascular wall of the small pulmonary artery (<50 μm in diameter) was noticeably thickened in the hypoxia-exposed mice (data not shown). The thickening of the small pulmonary artery is a well-known feature of the muscularized artery, associated with pulmonary hypertension [31]. These results indicate that hemodynamic stress has been generated under normobaric hypoxia employed in the present study.

Using the same model of the normobaric hypoxia, we analyzed the expression profiles of L-PGDS mRNA and protein in the heart and the testis (Fig. 1). The testis, enriched with L-PGDS, was included as a positive control for Northern and Western blot analyses. The expression of L-PGDS mRNA in the heart tended to increase under hypoxia and reached the higher levels after 14 days, compared with the control level on 1 day under normoxia and with the level of age-matched control mice kept under normoxia (Fig. 1A). Likewise, the expression levels of L-PGDS protein were increased in the heart after 14 days of hypoxia (Fig. 1B). The time-dependent change in L-PGDS protein level is largely paralleled with that in L-PGDS mRNA level. In contrast, there were no significant changes in the expression levels of L-PGDS mRNA and protein in the testis during hypoxia (Fig. 1C and D). These results suggest that the induction of L-PGDS expression in the heart may be a consequence of hemodynamic stress generated by chronic hypoxemia. The increased expression of L-PGDS in the heart may reflect the adaptation to the pressure overload. It should be noted that a certain amount of L-PGDS protein might be secreted into circulation, as reported in angina patients [10,12]. Incidentally, the time-dependent increase in L-PGDS protein parallels to the induction of HO-1 mRNA and protein in the heart under normobaric hypoxia [24].

Immunohistochemical analysis of L-PGDS in the myocardium

To identify the localization of L-PGDS in the heart, we performed the immunohistochemical analysis. L-PGDS is localized in the myocardium of the auricles and ventricles (Fig. 2). After 28 days of hypoxia, L-PGDS was increased in the left and right auricles (Fig. 2A and B) and ventricular myocardial cells (Fig. 2C and D). However, we were unable to detect the difference in the expression levels of L-PGDS between left and right ventricles.

Moreover, the immunoreactive L-PGDS was increased in the pulmonary venous myocardium after 28 days of normobaric hypoxia, compared with the normoxia-exposed mice (Fig. 3). It is noteworthy that L-PGDS is increased in the pulmonary venous myocardial cells. The pulmonary venous myocardium represents the extension of atrial myocardium into the vascular wall of the pulmonary vein [32,33]. These results suggest that the pulmonary vein is not a simple conduit but is rather actively involved in the regulation of pulmonary circulation. In contrast, expression of L-PGDS protein was not detectable in the alveolar architectures (Fig. 3) and the pulmonary artery (data not shown).

Increased expression level of L-PGDS in the heart of HO-2$^{-/-}$ mice

To explore the mechanism for the induction of L-PGDS expression in the heart during hypoxia, we analyzed its expression in HO-2$^{-/-}$ mice, a model of chronic hypoxemia [17]. HO-2$^{-/-}$ mice, maintained under normoxia, manifest mild hypoxemia and blunted hypoxic ventilatory responses, suggesting the impaired function of oxygen sensing. In addition, HO-2$^{-/-}$ mice exhibit the hypertrophy of the pulmonary venous myocardium [17], which re-

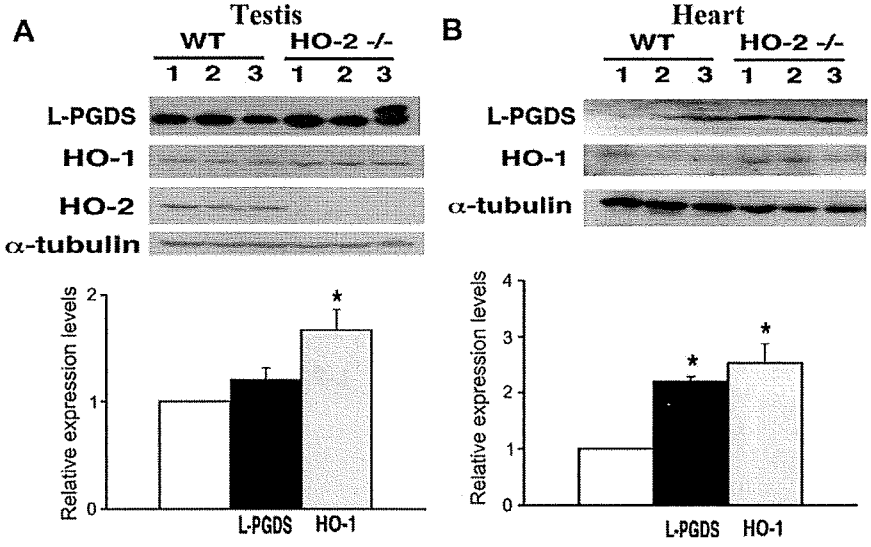

Fig. 4. Increased expression level of L-PGDS protein in the heart of HO-2$^{-/-}$ mouse. Tissue extracts were prepared from the testis (A) and the heart (B) of wild-type mouse (WT) and HO-2$^{-/-}$ mouse (HO-2$^{-/-}$), and analyzed by Western blot analysis with anti-mouse L-PGDS antibody, anti-HO-1 antibody or anti-HO-2 antibody (top panel, $n = 3$). Each lane contains 20 μg protein. Note that HO-2 protein was undetectable in the HO-2$^{-/-}$ mouse testis. To normalize the expressions levels of L-PGDS and HO-1 proteins, the same filter was used for anti-α-tubulin antibody. The intensity of the signals in the Western blot was normalized with respect to the intensity for α-tubulin. The relative expression level of L-PGDS or HO-1 protein indicates the ratio of each normalized value to that of L-PGDS or HO-1 protein in the wild-type mouse (open column). Asterisks represent significant difference compared to the respective control ($^*p < 0.05$).